Journal of Membrane Science 363 (2010) 87–95

Contents lists available at ScienceDirect

Journal of Membrane Science

journal homepage: www.elsevier.com/locate/memsci

Corn syrup clarification by microfiltration with ceramic membranes

Cristina Almandoz [a], Cecilia Pagliero [b], Ariel Ochoa [c], José Marchese [c,*]

[a] Inst. Multidisciplinario de Inv. Biol. de San Luis – IMIBIO (UNSL-CONICET), Chacabuco 917, 5700 San Luis, Argentina
[b] Departamento de Tecnología Química-Facultad de Ingeniería (UNRC-CONICET), Ruta 36, Km 601, 5800 Río Cuarto, Córdoba, Argentina
[c] Instituto de Física Aplicada – INFAP (UNSL-CONICET), Chacabuco 917, 5700 San Luis, Argentina

ARTICLE INFO

Article history:
Received 18 December 2009
Received in revised form 2 July 2010
Accepted 10 July 2010
Available online 16 July 2010

Keywords:
Microfiltration
Corn syrup
Clarification
Ceramic membrane
Membrane fouling

ABSTRACT

The performance in clarifying corn syrup of three different microfiltration ceramic membranes made in our laboratory was investigated. From preliminary MF tests at laboratory scale, it was found that the composite ceramic membrane with average hydraulic pore size radius of $r_h \approx 0.5\,\mu m$ (CM05) performed better than the other two membranes ($r_h \approx 0.14\,\mu m$ and $r_h \approx 0.75\,\mu m$). Further studies of corn syrup clarification with the CM05 membrane at bench scale, with and without air backpulsing, were performed. The effects of transmembrane pressure ($\Delta p = 10.3–103.4$ kPa) and the feed flow velocities ($v = 1.32–3.18$ m/s) on permeate flux at $T = 60\,^{\circ}C$ were analyzed. Permeate fluxes without back-flushing decreased considerably during the first hour of operation; around 60–70% of the initial permeate flux. Membrane fouling responsible for the permeate flux decline during the operation time was evaluated by applying different blocking models and cake filtration model. Results indicate that a good fitting correlation between the experimental data and pore blocking models was achieved. When back-flushing procedure was applied high efficiency of average permeate flux ($J \approx 95–105\,L/m^2\,h$) was obtained. From these experiments, sequential back-flushing is recommended to achieve the highest flux values and allow the filtration cycle to continue over longer periods of time. The turbidity, insoluble residue, and total protein rejection performances of CM05 membrane were significantly higher than those obtained using the traditional rotary vacuum filtration (RVF) process.

1. Introduction

The starch processing industry is characterized by streams that vary in diversity and complexity and that require extensive processing to achieve high end product quality. Water removal and product separations are two fundamental processing steps that impact on product quality and processing economics. Several membrane technologies have been used in the starch processing industry; these include pretreatment of fresh water, recovery of solids and wastewater treatment [1]. In corn wet milling, dry matter can be separated from liquids in process streams with centrifuges or vacuum belt filtration (VBF). Products that are industrially obtained from corn include fructose, glucoses, syrups mixture, maltose, dextrose, regular and modified starches, maltdextrin, candy dye, adhesives, dextrin, oils and gluten. These products are raw materials for the processes of a wide range of industries, such us, the food and pharmaceutical. Dextrose syrups are commercially produced from processes catalyzed by acids, acids–enzymes or enzymes–enzymes. Following conversion by acid/or enzyme hydrolysis of starch, corn syrup must be clarified to remove undesired oil, proteins and other non-starch components, commonly known as "mud". Downstream carbon adsorption and ion exchange remove color and reduce ash content. Traditionally, most of the non-desired components are precipitated, followed by centrifugation and/or diatomaceous earth, rotary vacuum or pressure leaf filtration. This requires a careful pH control and yields turbid syrup because neither technique can remove all of the mud. Rotary vacuum filtration also produces large quantities of spent filter aid, a significant waste disposal problem, and both processes have high maintenance cost [2,3].

The use of membrane is an interesting alternative to the conventional methods of clarification in the processing of syrup corn juice. Processes with membranes have been consolidated in various area of food production, being the separation process a non-thermal system, without phase changes or addition of chemical agents. The introduction of this technology in the food industry represents a technological solution to the problem of the production of juices with high quality, natural taste, and free of additives. In particular the microfiltration (MF) and ultrafiltration (UF) represent a valid alternative to the use of traditional coagulant agents (such as gelatin, bentonite, and silica) which effluents cause problems of environmental impact. In addition, the MF technique improves the microbiological quality of the permeate juice [4]. Thompson et al.

* Corresponding author. Tel.: +54 2652 424689; fax: +54 2652 430224.
E-mail addresses: marchese@unsl.edu.ar, marchese@termo.uva.es (J. Marchese).

0376-7388/$ – see front matter © 2010 Elsevier B.V. All rights reserved.
doi:10.1016/j.memsci.2010.07.017

[5] demonstrated that microfiltration has potential for separation of light and heavy gluten streams.

The most widespread commercial membranes are made from synthetic polymers or inorganic materials; hence they are classified as polymeric or inorganic membranes. In the second case, UF and MF inorganic membranes from ceramic materials (alumina, silica, kaolin, clay, zirconia, etc.) have been used in several juice clarification processes. Vladisavljević et al. [6] analyzed the variation of permeate flux with time filtration and the effect of operating pressure and feed flow rate during ultrafiltration of apple juice using ceramic membrane. Alumina ceramic tubular MF membrane with mean pore size of 0.2 μm was found to be suitable to clarify raw soy sauce [7]. This study showed that more than 99% of bacteria could be removed from raw soy sauce. Nandi et al. [8] studied the applicability of low cost ceramic membrane for mosambi juice microfiltration. The performance of ceramic membranes in clarifying limed and partially clarified raw sugar cane juice was investigated by Jegatheesan et al. [9]. These authors showed that the ceramic membrane tested with 0.05 μm pore size performed better than the other two membranes (pore sizes 0.02 and 0.1 μm). Recently [10], raw rice wine was clarified by MF using tubular ceramic membranes with various pore sizes and materials. The most suitable membrane was a 200 nm ZrO_2 membrane, which removed more than 90% of the insoluble fine particles (turbidity).

The use of microfiltration technique for corn syrup clarification with ceramic membranes has successfully been applied [11,12]. The microfiltration process applied to the clarification of these syrups has advantages over the conventional process because it replaces the use of diatomaceous earths reducing production costs [13–15]. The quality of clarified syrups by microfiltration membranes may be higher in terms of turbidity, color and microbiological cleaning compared with those produced by conventional filtration.

However, the main drawback of microfiltration ceramic membranes is the modifications of their structural properties due the fouling resulting in a significant decrease of the permeate flux, which in turn reduces the membrane productivity and life time. Several models have been used to describe solute fouling, among them hydraulic resistance, osmotic pressure, gel polarization, pore blocking and film models [16–18]. Hermia [19] revised the different blocking mechanisms and reformulated all of them in a common frame of power-law non-Newtonian fluids. Based on resistance-in-series model, Li et al. [7] investigated the effect of membrane microstructure and operational conditions on fouling behavior of ceramic membranes during microfiltration of raw soy sauce. Results showed that total resistance and concentration polarization resistance increase strongly with increasing nominal pore size while cake resistance and internal fouling resistance decrease slightly. The decline in permeate flux during the mosambi juice microfiltration [8] was analyzed using different membrane pore blocking models. Results showed that fouling resistance was about 85% to the total resistance for centrifuged mosambi juice and about 50% for enzyme treated centrifuged mosambi juice. Jegatheesan et al. [9] interpreted their membranes fouling by different blocking-cake fouling models and the combination of external and progressive internal fouling model. Li et al. [10] used three modified fouling models to describe flux decline behavior during the raw rice wine microfiltration. Analysis by the models indicated cake filtration to be the dominant mechanism and pore constriction to be the secondary fouling mechanism.

Several physical and chemical methods have been proposed for reducing membrane fouling during the microfiltration process, including hydrodynamic methods, chemical cleaning, modification of feed chemical properties, membrane surface modification, periodic backpulsing with water or air, etc. [20,21]. Backpulsing is employed in most microfiltration systems as an effective technique to destroy the cake layer, to remove deposited foulants from the membrane surface, and it also helps in preventing particles and macromolecules penetration into the membrane pores. Several research groups have investigated the use of backpulsing with ceramic membranes. Some of them have aimed on establishing the optimal backpulsing conditions during the microfiltration and ultrafiltration of different foulant solutions [22–27]. For example, Sondhi et al. [22,24] showed that backpulsing was effective in reducing the fouling phenomenon during their experiments filtering $Cr(OH)_3$ suspensions through porous alumina ceramic membranes. They reached up to fivefold increase in steady-state permeate flux and 100% flux recovery when forward filtration interval of 1.5 min and backpulse duration of 1 s were used. Mores and Davis [25] found that multiple short backpulses were more effective in cleaning the membrane surface than fewer, longer backpulses at high shear rate and backpulse pressure. Moreover, longer, weaker backpulses led to higher recovered fluxes than did shorter, stronger backpulses. Most of these research works have demonstrated the effectiveness of backpulse in reducing long-term membrane fouling while allowing the achievement of high product recovery.

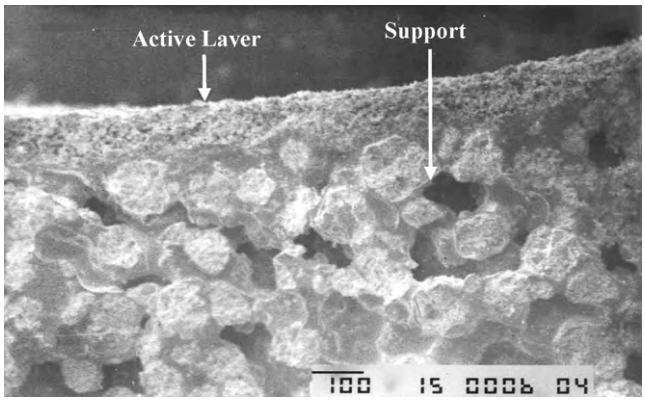

Fig. 1. Cross-section microphotograph of CM05 composite ceramic membrane.

This paper reports the results of an experimental study of corn syrup clarification using tubular microfiltration ceramic membranes prepared in our laboratory. Experiments were performed using corn syrup from a local factory. The effect of different experimental variables, i.e. the mean pore size of the active layer, feed flow, transmembrane pressure, and back-flushing on performance and quality of the clarified final syrup was analyzed. Experimental decay of permeate fluxes was interpreted in terms of the different pore blocking mechanism.

2. Experimental

2.1. Membranes

Three different tubular composite ceramic membranes (CM) with inner diameter ID ≈ 8 mm and outlet diameter OD ≈ 10 mm were used for the preliminary clarification syrup tests. Fig. 1 shows a representative SEM image of CM05 cross-section. Membranes are formed by an active layer (thickness 50–70 μm) of a substantially natural alumina-silicate material deposited on the inner surface of a tubular thick macro-porous ceramic support. The support and ceramic membranes were prepared controlling the paste formulation (clay, kaolin, alumina, feldspath and additives), particle size and thermal treatment. The green body was sintered at 1200 °C. Unsupported active layers (A01, A05, and A08) were prepared according with previous work [28]. The pore size distribution and porosity of support, active layers, and composite substrates (CM01, CM05, and CM08) were determined by the mercury penetration and pure water flux techniques [29]. The pore

Table 1
Structural parameters, hydraulic permeabilities, and fluxes of ceramic substrates.

Membrane	ε (%)	r_p (μm)	r_h (μm)	L_{h0} (L/h m^2 kPa)	J_0 (L/m^2 h)	J_∞ (L/m^2 h)
Support (S)	51.80	15.80	3.3	2760	–	–
A01	63.52	0.22	0.14	0.0055	–	–
A05	63.44	0.76	0.51	0.08	–	–
A08	62.91	1.32	0.75	0.16	–	–
CM01	51.53	1.54	–	9.84	77.5	25.6
CM05	55.10	2.07	–	46.63	136.2	28.5
CM08	53.93	15.50	–	273.45	175.7	32.3

size distribution analysis of mercury porosimetry measurements and AFM surface topographic images for unsupported active layers showed that [28,29]: (i) the A01 active layer had narrow distribution (pore size between 0.1 and 0.2 μm) with only a significant peak; (ii) A05 and A08 actives layers had a clear bimodal distribution with a broad pore size distribution ranging from 0.2 to 1.1 μm and 0.3 to 4.0 μm respectively; (iii) the three active layers had a high surface roughness and its value increased as the mean pore size increased (A08 > A05 > A01). The porosity (ε), hydraulic permeability (L_h), and mean pore radii from both volume mercury penetration (r_p) and water flux measurements (r_h) of the support, active layers and composite membranes are tabulated in Table 1.

2.2. Corn syrup

Turbid and clarified corn syrups were provided by Glucovil San Luis Plant (Ledesma S.A.A.I., Argentina). Clarified corn syrup was obtained by clarifying the original turbid syrup by the rotary vacuum filtration (RVF) technique at T = 60 °C using diatomaceous earth and activated carbon as filtration cake. The original corn syrup properties at T = 60 °C were density ρ = 1.04 g/ml (DMA35 Anton Paar densimeter); 20°Brix (Index Instrument refractometer); viscosity $\mu = 6.5 \times 10^{-3}$ cP (LV Brookfield viscometer).

2.3. Syrup physicochemical parameters

The following physicochemical parameters of syrups were evaluated: insoluble residues, total proteins, and turbidity. The separation efficiency of microfiltration membranes was determined by the observed rejection factor defined as:

$$R\% = \left(1 - \frac{C_p}{C_f}\right) 100 \quad (1)$$

where C_p and C_f are the permeate and feed concentration parameters respectively.

Insoluble residues: The content of insoluble residues was determined by weighting 200 g of corn syrup sample. The sample was filtrated with a previously weighted filter paper. After that, the liquid was removed by vacuum filtration. The remained solids and the filter paper were dried in a vacuum oven at T = 110 °C during 1 h. The dry filter paper with syrup residue was weighted and the percent of insoluble residue was determined.

Total proteins: Total protein concentration was determined as total nitrogen using the Kjeldahl method [30].

Turbidity: Syrup turbidity was determined by the turbidimitry technique using a UV Hitachi Spectrophotometer (U-2001). To obtain the calibration curve, samples of barium sulfate at different concentrations were prepared and their absorbencies at a wavelength of 420 nm were measured [31]. The absorbance of both, permeate and feed syrup samples was measured at 420 nm and their turbidity was expressed as barium sulfate concentration.

2.4. Syrup clarification experiments

2.4.1. Lab-scale microfiltration tests

Preliminary MF tests at laboratory scale were done to determine the membrane performance on permeate syrup flux and physicochemical characteristics. The experimental microfiltration device at lab scale has been described elsewhere [32]. The microfiltration experiments were carried out using composite tubular membranes with a length ℓ = 0.2 m and an inner transfer area of $A = 5.03 \times 10^{-3}$ m^2. The ceramic membrane was placed in an appropriated module made of acrylic material. The syrup was pumped through the inner side of the membrane using a peristaltic pump. The operational conditions, feed flow rate $v = 0.5$ m/s, transmembrane pressure Δp = 50 kPa, and the temperature T = 60 °C were kept constant.

2.4.2. Bench-scale microfiltration experiments

A schematic diagram of the retentate recycle bench-scale microfiltration unit operated in this study is shown in Fig. 2. The unit included three tubular microfiltration ceramic membranes placed in an acrylic housing. The length of each ceramic membrane was of 0.5 m and the internal effective total membrane transfer area was 0.0365 m^2. The same membranes were used for all the experiments. Forty liters (40 L) stainless steel tank (thermostatic bath Haake Mod. DL30-W46B) was used as reservoir of the feed-retentate corn syrup. The variable parameters analyzed in the microfiltration performance experiments were the feed crossflow and the transmembrane pressure. All the experimental runs were carried out at T = 60 °C according with the industrial RVF clarification process. Pressure and temperature measurements were obtained from the pressure gauge and the thermocouple located at the membrane retentate outlet. The syrup was pumped through the inner side of the membranes using a magnetic impeller pump (Pacific Scientific). Each experimental run was carried out during approximately 3 h with total retentate recycling. The operating pressures (10.3–103.4 kPa) and the feed flow velocities (v = 1.32, 2.31, and 3.18 m/s) were kept constant by the pump controller and the needle valve located in the outer string. The recycle retentate flow was measured with a flowmeter and the permeate flux was determined by time weighing the permeate syrup. An analytical balance interfaced with a computer was used to collect and to process the mass data of permeate versus time. The separation efficiency of MF ceramic membranes was determined by the rejection factors.

2.4.3. Back-flushing and membrane cleaning

Ceramic membranes were reused after each microfiltration experiment at bench scale. In order of both, to reach the initial membrane water flux and to improve the amount of permeate syrup flux, a back-flushing system was incorporated to the membrane module. This system consists of two electro-valves (E1 and E2) connected to a high N_2 pressure reservoir (Fig. 2). The experimental back-flush cleaning was carried out by filling up the membrane module with pure water and then applying into the permeate side a gas counter-pressure of 130 kPa during

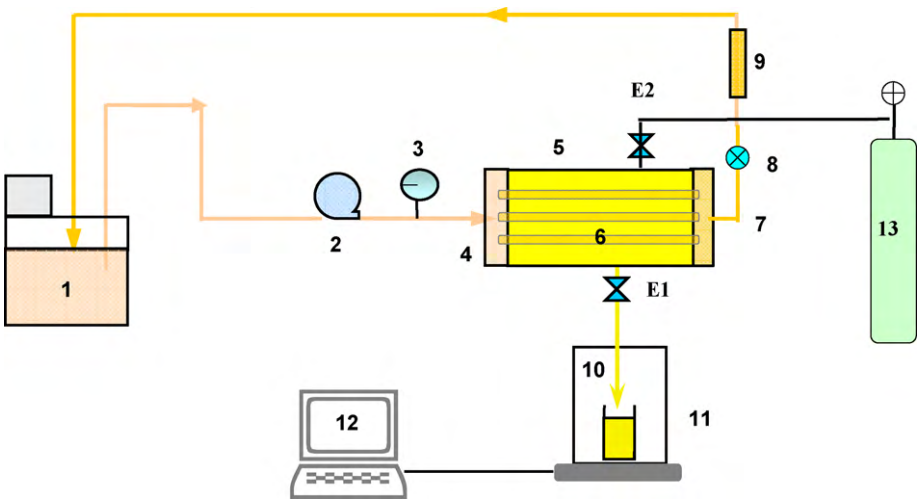

Fig. 2. Schematic representation of the bench-scale microfiltration device: (1) feed-retentate reservoir (thermostatic bath); (2) peristaltic pump; (3) gauge pressure; (4) feed syrup inlet; (5) membrane module; (6) ceramic membranes; (7) retentate outlet; (8) needle valve; (9) flowmeter; (10) permeate outlet; (11) balance; (12) data acquisition; (13) gas reservoir; E1 and E2 electro-valves.

5 min. In the backpressure operation the E1 electro-valve located at the permeate outlet module was automatically locked and the E2 electro-valve was simultaneously opened allowing the admission of N_2 gas into the permeate side pushing back a given permeate volume in the opposite direction. To complete the cleaning procedure, membranes were located in a ceramic oven at 300 °C during 1 h and then rinsed with pure water following the same back-flush procedure above mentioned.

3. Results and discussion

3.1. Lab-scale microfiltration tests

The hydraulic permeability, permeate flux, and the permeate quality were the main criteria to select the membrane to be used at bench scale. Fig. 3 shows the decline of syrup permeate fluxes for the composite ceramic membranes (CM01, CM05, and CM08). As shown this figure, a continuous decline in permeate fluxes was observed within the first hour. Afterwards, the permeate fluxes started to be stabilized reaching the pseudo steady-state (J_∞). The initial permeate fluxes (J_0) were evaluated from the initial corn syrup flux after 1 min of passing through the ceramic membrane. J_0 and J_∞ values for each experimental run are shown in Table 1. Table 2 resumes the physicochemical parameters of the original turbid syrup and the permeate syrup obtained after microfiltration with CM08, CM05 and CM01 composite ceramic membranes. For comparative reasons the quality parameter values of the clarified syrup obtained from diatomaceous earth rotary vacuum filtration are also given in Table 2. Reported data showed that the permeated syrups exhibited similar transparency and low color (high turbidity rejection factor). The results indicated that the CM05 and CM01 insoluble residue rejection ($R_{IR} \approx 99.6\%$) and total protein rejections ($R_{TP} = 80\%$) performance were significantly higher

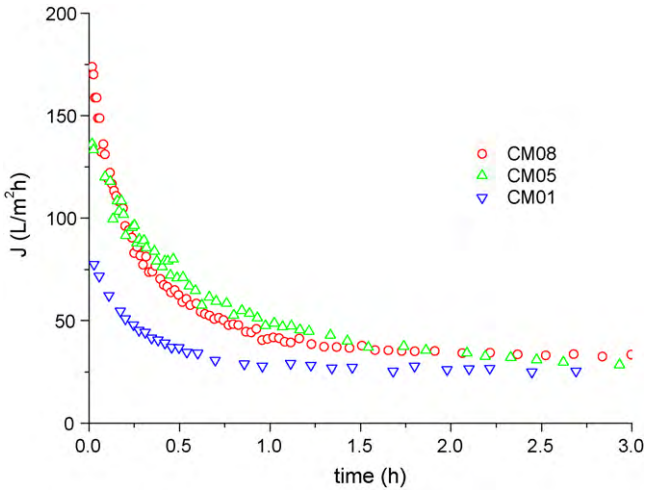

Fig. 3. Experimental flux decline of composite ceramic membranes at $v = 0.5$ m/s and $\Delta p = 50$ kPa (lab scale).

than those obtained with the traditional RVF process ($R_{IR} = 36.8\%$ and $R_{TP} = 70\%$) and with the CM08 membrane ($R_{IR} = 63.9\%$ and $R_{TP} = 71\%$).

The CM05 membrane performed better than the CM01. The CM05 had hydraulic permeability of $L_{h0} = 46.63$ L/h m^2 kPa and yielded initial and steady-state syrup fluxes of $J_0 = 136.2$ L/m^2 h and $J_\infty \approx 28.5$ L/m^2 h, while the values of CM01 membrane were lower ($L_{h0} = 9.84$ L/h m^2 kPa, $J_0 = 77.5$ L/m^2 h, and $J_\infty \approx 26$ L/m^2 h). From this analysis, it can be seen the CM05 membrane showed the highest efficiency for corn syrup clarification combining higher permeate flux and better clarified juice quality; so then, this membrane was chosen for further clarification studies at bench scale.

Table 2
Corn syrup physicochemical characteristics from: original, RVF, and permeate (lab scale).

Membrane	Syrup sample	Turbidity		Insoluble residues		Total proteins	
		g/L $BaSO_4$	$\%R_T$	% w/w	$\% R_{IR}$	% w/w	$\% R_{TP}$
	Original (feed)	1.343		0.332		0.1	
	RVF	0.03	97.8	0.21	36.75	0.03	70
CM08	Permeate	0.0325	97.6	0.12	63.85	0.029	71
CM05	Permeate	0.005	99.6	0.0009	99.75	0.02	80
CM01	Permeate	0.0346	97.4	0.0014	99.56	0.02	80

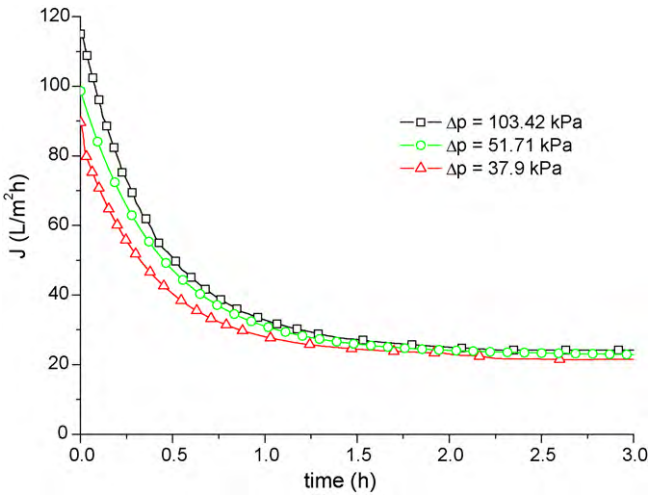

Fig. 4. Permeate flux time dependence of CM05 membrane at different transmembrane pressures and $v = 2.31$ m/s (bench scale).

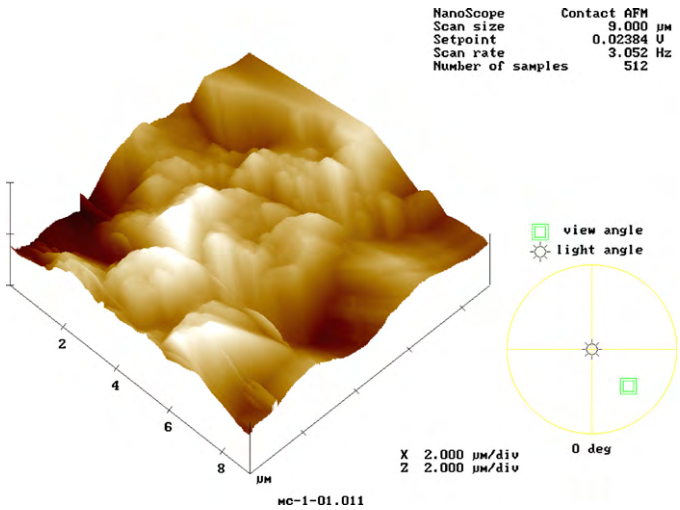

Fig. 5. Three-dimensional topographic AFM image of CM05 membrane surface.

3.2. Bench-scale corn syrup clarification

During the corn syrup clarification tests, the collected permeate mass data were processed as volume of accumulated permeate versus time. To obtain the permeate flux (J, L/m^2 h) at different operational times, incremental volume–time data were fitted with an exponential expression and it was then derived. The fitted J data as a function of time at feed flow rate $v = 2.31$ m/s and different pressures are reported in Fig. 4. Similar flux decline behavior from other experimental runs ($v = 1.32$ m/s and $v = 3.18$ m/s) was obtained. For all the runs the permeate flux decreased considerably during the first hour and after 2 h it practically remained constant (pseudo steady-state). This behavior implies that the membrane resistance changes during the microfiltration fouling. The decrease in flux with the operational time can be caused by several factors, such as concentration polarization, adsorption, pore blocking, development of a protein gel-layer at the membrane surface, etc. Table 3 summarizes the initial and the steady-state fluxes at different operational conditions. The rejection values of clarified syrup (turbidity, insoluble residues and total proteins) are also reported in the foot-note of Table 3. As it was expected, the experimental data showed that the permeate syrup at bench scale exhibited the same physicochemical properties than those obtained at lab scale (Table 2). These results confirm that the corn syrup quality obtained from CM05 microfiltration process was significantly higher than that from traditional RVF process.

After each cleaning procedure, the hydraulic permeabilities (L_h at $T = 25\,^\circ$C) of the treated membranes were evaluated. From Table 3 it can be observed that L_h values of the treated membranes were similar ($L_h = 36.4$–38.3 L/h m^2 kPa) and they were 15–20% lower than the hydraulic permeability of the original membrane ($L_{h0} = 45$ L/h m^2 kPa). This suggests that after the cleaning procedure the surface and/or the porous structure of the original membrane were slightly modified.

Table 3
Hydraulic permeability. Initial, steady-state, and normalized fluxes.

⟨v⟩ (m/s)	L_h (L/h m^2 kPa)	Δp (kPa)	J_0 (L/m^2 h)	J_∞ (L/m^2 h)	J_∞/J_0
1.32	[a]45.00	103.42	148.53	35.69	0.24
	38.30	51.71	139.64	33.82	0.24
	37.50	10.34	137.53	31.40	0.23
2.31	36.50	103.42	115.05	24.10	0.21
	36.33	51.71	98.55	22.86	0.23
	36.05	37.90	89.59	21.51	0.24
3.18	37.43	103.42	122.78	25.90	0.21
	36.45	51.71	98.68	22.07	0.23

Average rejections: turbidity $R_T\,\% \approx 99.6$; insoluble residues: $R_{IR}\,\% \approx 99.8$; total proteins: $R_{TP}\,\% \approx 80$.

[a] L_{h0}, hydraulic permeability of original membrane.

3.3. Membrane fouling interpretation

In general, the permeate flux increased with higher feed velocities, temperatures and pressures. The presence of solutes in the solvent leads to different flux behaviors with the applied pressure. In Table 3 the effect of transmembrane pressure on normalized permeate syrup fluxes (J_∞/J_0) at different crossflow velocities is showed. From these values it is clear that, no significant changes on the normalized fluxes are observed ($J_\infty/J_0 \approx 0.21$–$0.24$) when both, the transmembrane pressure and the feed flow velocity were changed. The transmembrane pressure behavior was found to be typical when the permeate flux is controlled by the mass transfer mechanism [33]. The non-reduction on fouling phenomena with the increased velocity could be in part attributed to the membrane surface roughness. Riedl et al. [34] have concluded that rough membranes produce a looser surface fouling layer that has a lower flow resistance per unit thickness of foulant than the dense fouling layers observed on smooth surface membranes. de Barros et al. [35], in their study of fouling interpretation in pineapple juice clarification, have assumed that the structure of ceramic membrane could possess many stagnant zones on the membrane surface where the feed turbulent flow would be unable to sweep away the accumulated solids.

As it was mentioned in Section 2.1, the synthesized ceramic membranes had a high surface roughness. Fig. 5 shows the AFM three-dimensional surface image of the A05 active layer [29]. This image shows a rough morphological structure, with cavities or valley zones formed by different particles size (clay, kaolin) bound each other. The distances between the surface maximum (peak) and minimum (valley) were around 1.5–0.5 μm. The high surface roughness of CM05 membrane could apparently be responsible of why higher crossflow velocities did not affect membrane fouling.

A decrease in flux is a rather complex phenomenon involving solute adsorption onto the membrane surface, pore blocking, concentration polarization, and cake layer formation. According to the early works on flux decline dynamics, fouling of porous membranes can be attributed to several more or less independent but generally coexisting phenomena. In any case the permeate flux time depen-

dence can be summarized by the following differential equation [16]:

$$-\frac{dJ}{dt} = k(J - J_\infty)J^{2-n} \quad (2)$$

k stands for a phenomenological characteristic coefficient, and n is the general index. The n parameter has different estimated values that depend of each fouling mechanism during the filtration process as follows:

- If $n = 1.5$ the fouling mechanism is know as "standard blocking model". The particles or different molecules of the solution are directly adsorbed on the pore walls. In this case there is a continuous decreasing of permeate flux with the operation time. This fouling phenomena always operates in non-steady-state condition ($J_\infty = 0$) and it is independent of the crossflow rate. The mathematical expression of J is

$$J^{-1/2} = J_0^{-1/2} + k_1 t \quad (3)$$

  where the parameter k_1 is related to the pore area reduction and the initial number of pores per surface unit.
- If $n = 1$, the fouling mechanism is so-called "intermediate blocking". This fouling occurs when the size of the solute particles are similar to the membrane pore size. In this model, it is assumed that a membrane pore is not necessarily blocked by the solute particles and some particles may settle over others. Therefore, the non-blocked membrane surface area diminishes with time and some particles are expected to obstruct the membrane pore entrance without blocking the pore completely. The flux expression is given by

$$J^{-1} = J_0^{-1} + k_2 t \quad (4)$$

  where the k_2 parameter can be related to the membrane blocked surface per unit of filtered volume.
- If $n = 2$, the fouling mechanism corresponds to the "complete blocking model", which assumes that each particle or solid compound that reaches the membrane surface plug completely the pore. The pore blocking takes place on the membrane surface and not inside the pores (the solute is larger than pore size). The equation that governs this model is

$$\ln J = \ln J_0 - k_3 t \quad (5)$$

  The k_3 parameter is related to the number of pores per surface unit blocked per unit of filtered volume.
- When $n = 0$, "cake filtration model", in this case the solute molecules are deposited and accumulated on the external membrane surface. The solid or macromolecules particles do not enter the pores and they form a boundary layer resistance or cake on the membrane surface. In this case:

$$J^{-2} = J_0^{-2} + k_4 t \quad (6)$$

  The k_4 parameter is related to the apparent specific resistance of the cake and to the cake mass per unit of permeated volume.

Attending to: (i) the high both, flux decline and rejection factor values ($R\% \approx 80$–99.8), (ii) the wide pore size distribution of the CM05 active layer, (iii) the solutes of different molecular weights contained in the corn syrup (starch, proteins, polysaccharides, etc.), it seems reasonable to assume that the resulting fouling should probably started with simultaneous pore blocking mechanisms and then cake fouling.

From these assumptions, the criterion it has been used in the theoretical interpretation of the flux decline was to fit only those experimental data included within the interval of time in which the correlation coefficients were higher than 0.99. The comparison between the best numerical predictions ($n = 0$, 1, 1.5, and 2) and

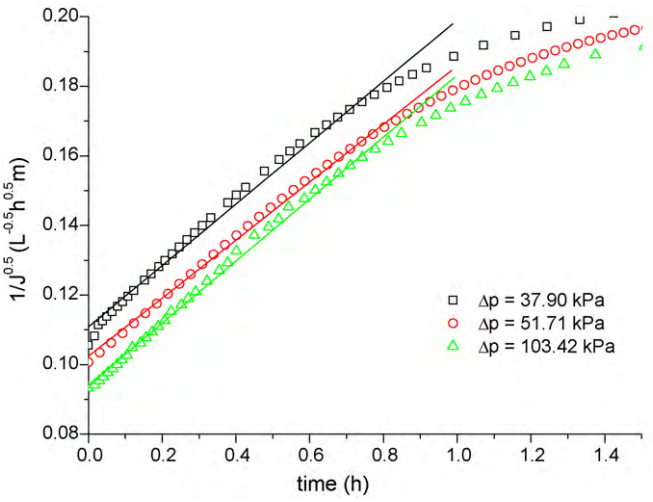

Fig. 6. Standard blocking fouling model fitting (straight lines) to the experimental data (symbols) at $v = 2.31$ m/s.

experimental data at $v = 2.31$ m/s and different transmembrane pressures are shown in Figs. 6–9. Figs. 6 and 7 show the good fitness of the experimental data, in the time interval of 0–60 min, for the standard and intermediate models according to Eqs. (3) and (4). In Fig. 8 a plot of $\ln J$ versus time (Eq. (5)) is shown. This representation should give a straight line when the complete blocking is the more important fouling mechanism. It can be seen that this is effectively the case for operational time between 0 and 30 min approximately. On the other hand, cake formation mechanism (Eq. (6)) predominated at time interval ranging from 60 to 180 min as it can be observed in Fig. 9. The same fitting procedure was applied for the experimental runs at $v = 1.32$ m/s and $v = 3.18$ m/s. In Table 4, the corresponding parameters values of k constants and initial flux (J_0) by fitting experimental data with fouling models are tabulated. The difference among the k values at different transmembrane pressures and crossflow velocities were very low. The so obtained k values do not follow the expected trend, increase as the transmembrane pressure increases. This could be probably attributed to the same fouling behavior and to the similar steady-state fluxes values at different operational conditions. Referring to the extrapolated initial flux from the complete blocking model, they were very close to the experimental data (within 99–92%). In spite of the

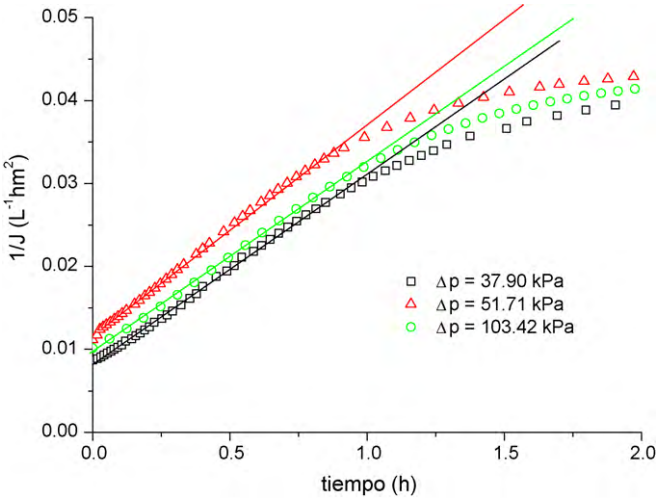

Fig. 7. Intermediate pore blocking fouling model fitting (straight lines) to the experimental data (symbols) at $v = 2.31$ m/s.

Table 4
k and J_0 parameter values of different fouling mechanisms (correlation coefficients $R^2 \geq 0.99$).

⟨v⟩ (m/s)	Δp (kPa)	J_0 exp (L/m² h)	Standard blocking		Intermediate blocking		Complete blocking		Cake fouling	
			J_0	$k_1 \times 10^2$	J_0	$k_2 \times 10^2$	J_0	k_3	J_0	$k_4 \times 10^4$
1.32	103.42	148.53	138.37	3.93	146.84	0.88	145.52	1.01	75.27	2.02
	51.71	139.64	136.54	4.20	143.47	0.93	138.97	0.96	–	3.12
	10.34	137.53	128.46	10.64	134.22	2.40	132.43	2.35	51.47	2.06
2.31	103.42	115.05	112.86	8.91	121.65	2.28	114.40	1.76	37.69	4.51
	51.71	98.65	95.29	8.33	102.35	2.55	96.39	1.48	28.86	2.61
	37.9	89.6	81.41	8.82	85.47	2.28	83.99	1.61	36.24	5.81
3.18	103.42	122.78	120.30	9.34	128.20	2.26	119.12	1.74	31.46	1.67
	51.71	98.68	86.53	15.01	87.61	3.94	90.85	2.93	26.92	2.22

J_0 (L/m² h); k_1 (L$^{0.5}$ m/h$^{1.5}$); k_2 (m²/L); k_3 (h^{-1}); k_4 (m⁴ h/L).

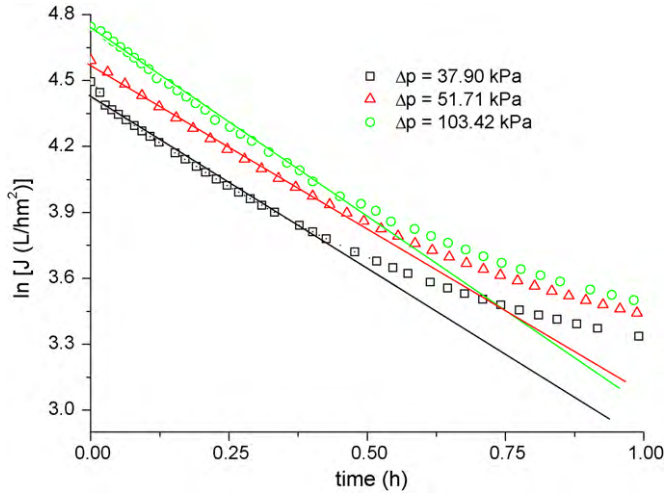

Fig. 8. Complete blocking fouling model fitting (straight lines) to the experimental data (symbols) at $v = 2.31$ m/s.

good data correlation given by the cake model, the extrapolated initial flux values obtained from this model are 50–73% lower than the experimental ones. Besides that, an imaginary number value of $J_0 = \sqrt{(-2.4 \times 10^4)}$ was obtained when the experimental data at $v = 1.32$ m/s and $\Delta p = 51.71$ kPa were fitted using the cake fouling model. These results suggest that the pore blocking fouling appears as the dominant mass transfer mechanism through the membrane. The pore blocking fouling can be mainly attributed to the structural characteristics of the CM05 membrane and to the solutes of different molecular weights contained in the corn syrup. While these mechanisms show a good data correlation, they undoubtedly oversimplify the several simultaneous coexisting phenomena involved during the permeate flux decay (solute–solute interactions, solute–membrane interaction, solute size exclusion, solute diffusion, shear effects, etc.).

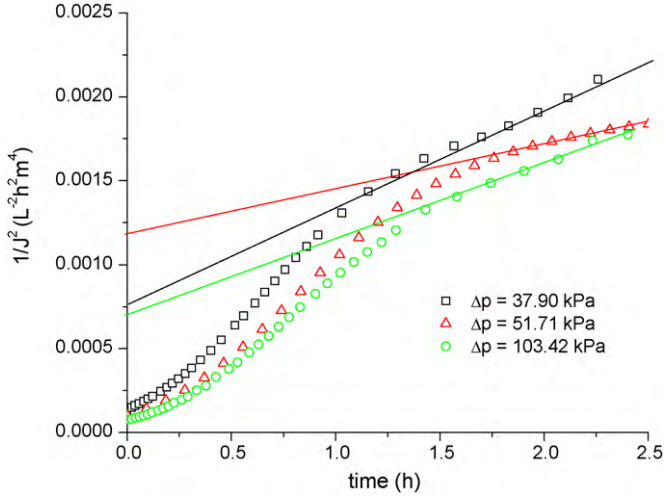

Fig. 9. Cake fouling model fitting (straight lines) to the experimental data (symbols) at $v = 2.31$ m/s.

Even if there are many studies in the literature related with the application of microfiltration technique for various juices, only few of them are related with corn syrup clarification. The corn syrup used in our clarification research (20°Brix, 60 °C) is comparable to the partially clarified sugar cane juice (16°Brix, 60 °C) used by Jegatheesan et al. [9]. In their clarification studies with ceramic membranes of different pore size (0.02, 0.05, and 0.1 μm) they have concluded that "cake filtration become dominant when the membranes have pore sizes in the ultrafiltration range where internal membrane pore blocking becomes insignificant" and "that the membrane that has pore size in the microfiltration range is susceptible to both external as well as progressive fouling". Their conclusions agree with the results obtained in the present work, where the structural characteristics of the membrane, broad pore size distribution (0.2–1.1 μm), high surface roughness and tortuous structure, together with the size and heterogeneity of the foulant molecules, would mainly produce a progressive pore blocking fouling.

3.4. Back-flushing performance

Crossflow filtration is often helpful in slowing down membrane fouling but does not eliminate it. Back-flushing can help removing the excessive particle deposits on the membrane surface and into the pores, minimizing the decrease in flux. It involves the application of periodic counter-pressure on the permeate side of the membrane to push a small quantity of permeate through the support into the feed of the module. It had been demonstrated [36] that for practical application back-flushing should start at the beginning of the filtration operation. The experimental back-flushing tests were applied at the highest transmembrane pressure ($\Delta p = 103.4$ kPa) and the three feed syrup crossflows ($v =$ 1.32, 2.31, and 3.18 m/s). Back-flushing was achieved by applying the following procedure: the electro-valves were set up to operate by reversing the permeate flux at the beginning of the filtration operation ($t = 3$ min) for a short interval of time: 5 s each 3 min with a gas counter-pressure of 130 kPa. During the backpressure operation the E1 electro-valve located at the permeate outlet module was automatically locked and the E2 electro-valve was simultaneously opened allowing the admission of N_2 gas into the permeate side during 5 s. Then the E1 was automatically opened and the E2 was simultaneously locked during 3 min, after that, the sequential back-flushing started again. Fig. 10 shows the average flux at different velocities after 2 h of operation resulting from sys-

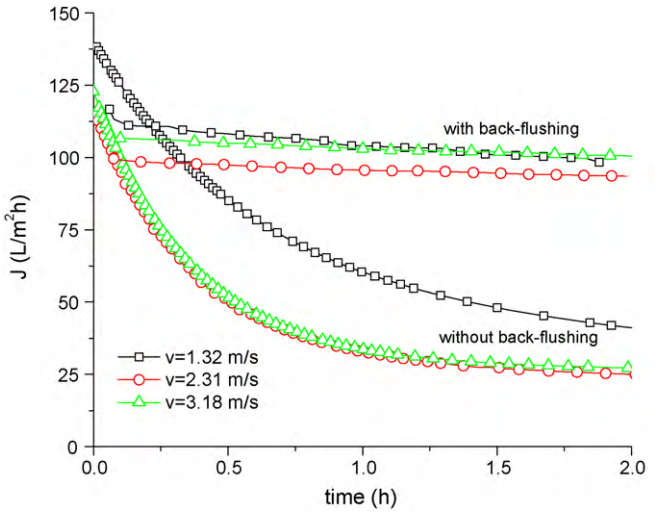

Fig. 10. Effect of sequential back-flushing (gas back pressure 130 kPa) on permeate flux at different crossflow velocities and $\Delta p = 103.42$ kPa.

tems with back-flushing procedure and the corresponding graph of flux without back-flushing. When no back-flushing is used the fluxes decreases from $J_0 \approx 115$–145 to $J_\infty \approx 24$–36 L/m^2 h and when back-flushing procedure was applied a high efficiency of average fluxes ($J_{av} \approx 95$–105 L/m^2 h) was obtained. These data showed the effectiveness of the back-flushing technique resulting in around fourfold increase in steady-state flux and 73–83% initial flux recovery. These results confirm that higher crossflow velocities do not affect membrane fouling and the average permeate flux was mainly controlled by the backpulsing technique. Although high average flux was obtained in the back-flushing procedure, there was a certain percentage loss of permeate associated with back-flushing due to counter-current permeation. The flux recovery due to sequential back-flushing far exceeded the percentage loss (below 3%) in the produced permeate. The quality of the permeate corn syrup with back-flushing was similar to that without back-flush.

In the clarification of limed and sugar cane with commercial ceramic membranes of different pore size Jegatheesan et al. [9] have demonstrated that intermittent air back-flushing only improved the performance of 0.1 μm membrane. The relatively low flux recovery (20–25%) compared with our back-flush results could be mainly attributed the membranes different pore sizes. The high flux recoveries obtained in our experiments are comparable to those results obtained by others researchers. Sondhi et al. [22] used Membralox® alumina membranes of various pore sizes (0.2, 0.8, and 5.0 μm) in their crossflow filtration experiments with chromium hydroxide suspension. The filtration experiments with and without backpulsing showed that backpulsing was effective in reducing the fouling phenomenon resulting in up to fivefold increase in steady-state flux and 100% flux recovery. They also concluded that the larger the pore diameter, the greater was the effectiveness of backpulsing. In the beer clarification by microfiltration, Gan et al. [23] investigated the effects of pore size using ceramic membranes (Ceramem) with nominal pore diameters of 0.2, 0.5, 1.3 μm. They found that enhanced surface hydrodynamics had very limited effect on improving flux. In the microfiltration back-flush experiments, after 24 h, the average flux was increased a 44.2% compared to normal crossflow filtration. Sondhi and Bhave [24] have established the importance of the role of backpulsing with experimental data on the bench scale, pilot scale and large-scale filtration systems using different Membralox® ceramic membranes and process streams. In their analysis the dependence of membrane cleaning time on backpulse parameters and membrane pore size were discussed. The backpulse effectiveness on some industrial applications was also discussed, among them: (i) filtration experiments of dilute yeast suspensions with 0.2 μm ceramic membrane, in which high flux of about 900 L/m^2 h can be maintained at backpulse interval of 1 min, (ii) slurry filtration with 0.05 μm tubular multichannel ceramic membrane. In this study the average flux increased a 20–25% at concentration factor of 40 (≈97.5% recovery) when the backpulse was applied, (iii) filtration of oily wastewater. It was showed that cleaning interval of the membrane could be extended to several months using a 0.8 μm membrane when flux values around 300 L/m^2 h were maintained by backpulse mode.

The above experimental results and analysis suggest that the low cost ceramic membranes prepared in our laboratory, operating in back-flushing mode, could be applied to the treatment of different types of industrial liquid suspensions (juice clarification, wastewater effluent, dairy products, etc.).

4. Conclusion

In this study, a thorough analysis of corn syrup clarification with microfiltration ceramic membrane is provided. Three microporous composite membranes with hydraulic mean pore sizes, r_h, of 0.75, 0.5, and 0.14 μm and total porosity between 51 and 55% were prepared from inexpensive regional alumina-silicate materials (clay, kaolin, feldspath, alumina, etc.). After preliminary clarification tests at lab scale the composite membrane CM05 ($r_h = 0.5$ μm) was selected for further studies at bench scale because its high both, hydraulic permeability and permeate juice quality.

Bench-scale clarification experiments of turbid corn syrup at different feed flow velocities and transmembrane pressures were performed. The experimental device included an air back-flushing system. Experimental decay of permeate fluxes was interpreted in terms of the pore blocking and cake fouling mechanisms. Although good correlations between the experimental data and theoretical fittings ($R^2 \geq 0.99$) with all models were achieved, pore blocking mechanisms (standard, intermediate, and complete) predicted initial fluxes more accurately than the cake model. These results suggest that the pore blocking fouling appears as dominant mechanisms of mass transfer through the membrane.

To reduce the membrane fouling effect on permeate flux decay an intermittent nitrogen gas back-flushing on the membrane permeate side was applied. This procedure allowed improving the performance of CM05 membrane during the clarification tests resulting in around fourfold increase in flux. From these results sequential back-flushing at the beginning of the filtration process is recommended to achieve higher flux values and to allow the microfiltration cycle to continue over longer periods of time.

It is worth mention that high solute rejections (80–99.8%) during the clarification test, with or without back-flushing, were achieved. These syrup quality results ratify the high filtration performance of the CM05 ceramic membrane.

The results of this research showed that low cost lab made microfiltration ceramic membranes are a reliable alternative for the conventional technology used in the corn syrup clarification and for promissory application in other industrial process streams.

Acknowledgements

The authors would like to thank FONCyT (Fondos para la Investigación Científica y Tecnológica) project PICT 2004-25482, and the Universidad Nacional de San Luis, PIP No. 2-8111.

References

[1] K.D. Rausch, Front end to backpipe: membrane technology in the starch processing industry, Starch/Stärke 54 (2002) 273–284.

[2] A.J. Basso, Vacuum filtration using filter aids, Chem. Eng. 89 (8) (1982) 159–160, 162.
[3] P.H. Blanchard, Technology of Corn Wet Milling and Associated Processes, Elsevier Science Publishers, New York, 1992.
[4] L. Carvalho, I. Castro, C. Bento da Silva, A study of retention of sugars in the process of clarification of pineapple juice (*Ananas comosus*, L. Merril) by micro- and ultra-filtration, J. Food Eng. 87 (2008) 447–454.
[5] C.I. Thompson, K.D. Rausch, R.L. Belyea, M.E. Tumbleson, Microfiltration of gluten processing streams from corn wet milling, Bioresour. Technol. 97 (2006) 348–354.
[6] G.T. Vladisavljević, P. Vukosavljević, B. Bukvić, Permeate flux and fouling resistance in ultrafiltration of depectinized apple juice using ceramic membranes, J. Food Eng. 60 (2003) 241–247.
[7] M. Li, Y. Zhao, S. Zhou, W. Xing, F.-S. Wong, Resistance analysis for ceramic membrane microfiltration of raw soy sauce, J. Membr. Sci. 299 (2007) 122–129.
[8] B.K. Nandi, R. Uppaluri, M.K. Purkait, Microfiltration of mosambi juice using law cost ceramic membrane, J. Food Eng. 95 (2009) 597–605.
[9] V. Jegatheesan, D.D. Phonga, L. Shu, R. Ben Aim, Performance of ceramic micro- and ultrafiltration membranes treating limed and partially clarified sugar cane juice, J. Membr. Sci. 327 (2009) 69–77.
[10] M. Li, Y. Zhao, S. Zhou, W. Xing, Clarification of raw rice wine by ceramic microfiltration membranes and membrane fouling analysis, Desalination 256 (2010) 166–173.
[11] N. Singh, M. Cheryan, Fouling of a ceramic microfiltration membrane by corn starch hydrolysate, J. Membr. Sci. 135 (1997) 195–202.
[12] X. Lancrenon, M.A. Theoleyre, G. Kientz, Mineral membrane filtration for the corn refining industry, Int. Sugar J. 96 (1994) 365–367.
[13] B. Keskinler, E. Yildiz, E. Erhan, M. Dogruc, Y.K. Bayhan, G. Akay, Crossflow microfiltration of low concentration-nonliving yeast suspensions, J. Membr. Sci. 233 (2004) 59–69.
[14] N. Singh, M. Cheryan, Process design and economic analysis of a ceramic membrane system for microfiltration of corn starch hydrolysate, J. Food Eng. 38 (1998) 57–67.
[15] F. Lutina, M. Baillya, D. Bar, Process improvements with innovative technologies in the starch and sugar industries, Desalination 148 (2002) 121–124.
[16] R.W. Field, D. Wu, J.A. Howell, B.B. Gupta, Critical flux concept for microfiltration fouling, J. Membr. Sci. 100 (1995) 259–272.
[17] L. Palacio, C.C. Ho, P. Prádanos, A. Hernández, A.L. Zydney, Fouling with protein mixtures in microfiltration: BSA–lysozyme and BSA–pepsin, J. Membr. Sci. 222 (2003) 41–51.
[18] M. Cinta Vincent Vela, S. Alvarez Blanco, J. Lora García, E.B. Rodríguez, Analysis of membrane pore blocking models applied to the ultrafiltration of PEG, Sep. Purif. Technol. 62 (2008) 489–498.
[19] J. Hermia, Constant pressure blocking filtration law: application to power law non-Newtonian fluids, Trans. I. Chem. Eng. 60 (1982) 183–187.
[20] G. Belfort, R.H. Davis, A.L. Zydney, The behavior of suspensions and macromolecular solutions in crossflow microfiltration, J. Membr. Sci. 96 (1994) 1–58.
[21] K.J. Hwang, H.C. Liu, W.M. Lu, Local properties of cake in cross-flow microfiltration of submicron particles, J. Membr. Sci. 138 (2) (1998) 181.
[22] R. Sondhi, Y.S. Lin, F. Alvarez, Crossflow filtration of chromium hydroxide suspension by ceramic membranes: fouling and its minimization by backpulsing, J. Membr. Sci. 174 (2000) 111–122.
[23] Q. Gan, J.A. Howell, R.W. Field, R. England, M.R. Bird, C.L. O'Shaughnessy, M.T. MeKechinie, Beer clarification by microfiltration—product quality control and fractionation of particles and macromolecules, J. Membr. Sci. 194 (2001) 185–196.
[24] R. Sondhi, R. Bhave, Role of backpulsing in fouling minimization in crossflow filtration with ceramic membranes, J. Membr. Sci. 186 (2001) 41–52.
[25] W.D. Mores, R.H. Davis, Yeast foulant removal by backpulses in crossflow microfiltration, J. Membr. Sci. 208 (2002) 389–404.
[26] A. Salladini, M. Prisciandaro, D. Barba, Ultrafiltration of biologically treated wastewater by using backflushing, Desalination 207 (2007) 24–34.
[27] K.-J. Hwanga, C.-S. Chan, K.-L. Tung, Effect of backwash on the performance of submerged membrane filtration, J. Membr. Sci. 330 (2009) 349–356.
[28] M.C. Almandoz, J. Marchese, P. Prádanos, L. Palacio, A. Hernandez, Preparation and characterization of non-supported microfiltration membranes from aluminasilicates, J. Membr. Sci. 241 (2004) 95–103.
[29] J. Marchese, C. Almandoz, M. Amaral, L. Palacio, J.I. Calvo, P. Prádanos, A. Hernandez, Fabricación y caracterización de membranas cerámicas tubulares para microfiltración, Bol. Soc. Esp. Ceram. Vidrio 39 (2) (2000) 1–10.
[30] AOAC Official method 979.09, Official Method of Analysis, Association of Analytical Communities, Washington, DC, 2002.
[31] Standard Method for the Examination of Water and Wastewater 17 Edition, SMEWW Part 4500-$SO_4^{=}$E. Spanish Version 1992.
[32] J. Marchese, M. Amaral, J. Encabo, C. Almandoz, Application of Ceramic Membranes to Slaughterhouse Wastewater Treatment, The Minerals, Metals & Materials Society. in: Gaballah, J. Hager, R. Solozabal (Eds.), vol. III (1999) pp. 2377–2385.
[33] M. Cheryan, Ultrafiltration Handbook, Technomic Publishing Company, Inc., Lancaster, PA, USA, 1986, pp. 76–85.
[34] K. Riedl, B. Girard, R.W. Lencki, Influence of membrane structure on fouling layer morphology during apple juice clarification, J. Membr. Sci. 139 (1998) 155–166.
[35] S.T.D. de Barros, C.M.G. Andrade, E.S. Mendes, L. Peres, Study of fouling mechanism in pineapple juice clarification by ultrafiltration, J. Membr. Sci. 215 (2003) 213–224.
[36] R.R. Bhave, Liquid filtration and separation with inorganic membranes, in: R.R. Bhave (Ed.), Inorganic Membranes: Synthesis, Characteristics, and Applications, Chapman & Hall, New York/London, 1991, pp. 129–154.